Desalination and Water Treatment
www.deswater.com

34 (2011) 156–162
October

1944-3994/1944-3986
doi: 10/5004/dwt.2011.2898

In-situ characterization of fouling layers: which tool for which measurement?

Patrick Loulergue[a,b,c,*], Cédric André[d], Didier Laux[d], Jean-Yves Ferrandis[d], Christelle Guigui[a,b,c], Corinne Cabassud[a,b,c]

[a]*Université de Toulouse; INSA, UPS, INP; LISBP, 135 Avenue de Rangueil, F-31077 Toulouse, France*
Tel. +33561559783; Fax: +33561559760; email: patrick.loulergue@insa-toulouse.fr
[b]*INRA, UMR792 Ingénierie des Systèmes Biologiques et des Procédés, F-31400 Toulouse, France*
[c]*CNRS, UMR5504, F-31400 Toulouse, France*
[d]*Université Montpellier II. Place Eugène Bataillon, IES, institut d'Electronique du Sud. CC082, 34095 FRANCE*

Received 3 September 2010; Accepted 3 January 2011

ABSTRACT

In the last decade, a number of methods have been developed for the in-situ characterization of fouling layers formed in confined geometry. Laser sheet at grazing incidence and ultrasonic time domain reflectometry are relevant methods to measure fouling layer thickness. However, these two methods have never been used simultaneously during the same filtration run. The objective of this study was to compare values measured by both methods. After validation of the thicknesses given by each method on an especially designed calibrated gauge, measurements were made simultaneously by both methods on porous fouling layers formed on two membranes with different permeabilities. The results show that, in the case of a compact fouling layer, the thicknesses given by the two methods are the same. However, for more porous layers, such as concentration polarization layers, thicknesses differ, although the growth kinetics is identical. Thus, laser sheet at grazing incidence and ultrasonic time domain reflectometry are two complementary methods to determine fouling layer thickness and/or its growth kinetics according to operating conditions.

Keywords: Particle deposit; In-situ measurement; Ultrasonic Time Domain Reflectometry; Structural properties; Laser Sheet at Grazing Incidence; Bulk suspension/deposit interface

1. Introduction

Understanding the mechanisms that lead to the formation of fouling layers is a key point to optimize process performance. In the last twenty years, a number of in-situ, non-invasive techniques have been developed and used to study fouling [1–7]. However, only a few of them can be applied to the study of fouling layers formed in confined geometry, such as in hollow fibre membranes. Among the methods allowing in-situ characterization of fouling layers formed in confined geometry, the laser sheet at grazing incidence method (LSGI) developed by Mendret and co-workers [4] and the ultrasonic time domain reflectometry (UTDR) method can be relevant.

The LSGI method determines cake layer thickness by monitoring the deflection of a laser sheet in time with the fouling layer growth. So far, this method has mostly been applied to determine thicknesses of bentonite cake layers formed on ultrafiltration membranes. The UTDR method was first applied to characterize fouling layers formed on flat sheet membranes by Mairal et al. [1]. More recently, several authors have demonstrated that this method is relevant to measure the thickness of kaolin or bentonite cake layers formed in confined spaces [5–6].

However, one can wonder if both methods give the same results when they are positioned on the same

*Corresponding author.

Presented at the AMS6/IMSTEC10, The 6th conference of the Aseanian Membrane Society in conjunction with the 7th International Membrane Science and Technology Conference, Sydney Australia, November 22–26, 2010

experimental apparatus and for the same fouling layer morphology. Thus, the objective of this study is to determine whether thicknesses measured simultaneously by the two methods are the same. That is to say, to determine if the nature of the interface between bulk suspensions and fouling layers is the same for both methods. First, in order to validate the thickness given by each method, measurements were performed by both methods for a specially designed calibrated test piece made of a continuous, rigid medium with a well defined interface. Secondly, measurements were carried out during filtration of a model particle suspension. Spherical monodispersed melamine particles were chosen for this work. Fouling layers with different morphologies were created during filtration using two different kinds of membranes with different permeabilities. The thicknesses of these fouling layers were determined simultaneously by both methods during the same filtration run.

2. Material and methods

2.1. Filtration cells

Two filtration cells were used. They were made of two parallel plates of Plexiglas with a narrow channel machined in the internal face of each plate. This rectangular channel had a length of 28.2 cm and a depth of 2 mm. One cell had a channel width of 4 mm, the other 2 mm. These dimensions were chosen in order to consider the confinement phenomena occurring in an inside/out hollow fiber. The cell with the larger channel was used for measurements on the calibrated test piece, while the cell with the narrower channel was used for filtration experiments. For filtration experiments, a flat sheet-membrane was placed between the two plates so that the filtration only occurred on the channel area (5.64×10^{-4} m²). More details are given elsewhere [8].

2.2. Calibrated test piece

First, in order to avoid having to consider the complex behavior of electromagnetic and ultrasonic waves in a porous medium, measurements were performed with a specially designed and machined PVC test piece. This material is rigid, continuous and has a well defined interface. To approach filtration conditions, the measurement of the test piece had to be performed in the filtration cell. Thus, it was designed in such a way that it could be placed in the 4 mm-wide filtration channel.

The test piece geometry had to be suited to the measurement methods. As the optical method is based on the deflection of a laser sheet due to the growth of a fouling layer, and because it was not possible to move either the laser sheet or the recording camera during the measurement, the test piece was designed with two notches of different depths along its length (Fig. 1). The notches are noted 1 and 3 in Fig. 1. Applying the LSGI method, the measured value was directly the thickness difference between notches 1 and 3.

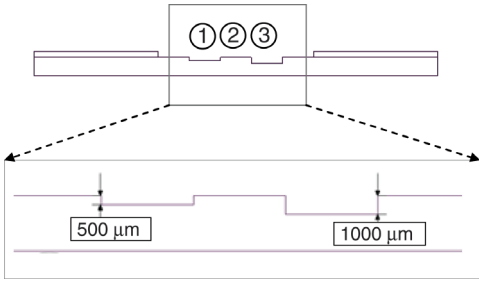

Fig. 1. Front view of the test piece and focus on the notches.

Using the acoustic method, it was possible to measure the thickness of the gauge at the location of each notch. Thus, by measuring the thicknesses at notches 1 and 3, it was possible to calculate the difference of thickness between the two notches by simple subtraction.

The notch depths given in Fig. 1 are the values fixed for the test piece machining. However, the thickness of the test piece determined by a sensor gauge was used as a reference to validate the methods.

2.3. Filtration experiment and membrane cleaning

Suspensions of monodispersed spherical melamine particles (Duke Scientific Corporation, USA) with a mean diameter of 513 nm were filtrated. The particles were not deformable at the working pressure (1 bar) and had a density of 1510 kg.m^{-3}. They were suspended in ultrapure water at a concentration of 150.0 ± 0.7 mg/l. Neither aggregation nor settling was observed in the feed suspension during filtration runs. Due to the presence of surfactant in the particle mother suspension, the pH was 4.3 and the conductivity was 12 µS.cm^{-1}. The zeta potential of a particle was 44.6 ± 1.1 mV.

Two different kinds of polyethersulfone ultrafiltration membranes (Novasep-Orelis, Fr) were used. One had a molecular weight cut-off of 100 kDa (dextran) while the other had a pore diameter of 0.01 µm. They had different initial permabilities of 360 l/h.m².bar and 62 l/h.m².bar and thus generated different convective flows during filtration at a given pressure. According to the pore and particle sizes, it was assumed that no internal pore blocking occurred and particle retention was total. Filtration experiments were performed in dead-end mode at constant transmembrane pressure of 1 bar.

At the end of each experiment, membranes were cleaned according to specific protocols. For the membrane with a pore size of 0.01 µm, a relaxation step (5 min)

was followed by a flush. As suggested by Bessiere et al., [9], a large amount of ultrapure water was circulated in the feed side of the filtration channel at low flow to avoid erosion of a deposit. In the case of the 100 kDa membrane, the flush step was then followed by a 30-minute backwash at a transmembrane pressure of 1.7 bar. Whatever the rinsing protocol, the membrane permeability was then measured and compared to the initial one.

2.4. Thickness measurement methods

2.4.1. Laser sheet at grazing incidence (LSGI)

The method used was the in-situ, real time, non-invasive technique developed by Mendret et al. [4] for cake layer characterization using a laser sheet at grazing incidence on a membrane. At the start of the experiment, the laser-sheet was placed at a grazing incidence on the membrane. Thus a contact line was made between the laser sheet and the clean membrane. When a cake is grew on the membrane surface, the laser beam was deflected from its original position. The measurement of this deflection versus time enabled the cake thickness to be estimated. More details concerning this method are given elsewhere [4].

Two different lenses with magnifications of 12 X and 24 X were used depending on the size of the surface to be characterized. The lens choice dictated the precision of the measurement as this is directly linked to the lens magnification. Thus, during the test-piece thickness measurement, the 12 X lens was used, leading to a measurement uncertainty of ±15%. During filtration runs, the 24 X lens was used, which enabled the uncertainty to be reduced to ±5%.

2.4.2. Ultrasonic time domain reflectometry (UTDR)

UTDR measurement is based on the behavior of ultrasonic waves when they meet an interface. The velocity of the wave depends on the physical properties (density) of the medium and, when the wave encounters an interface between two media, energy is partitioned and a reflected wave occurs. Using a transducer, it is possible to monitor the echoes created at various interfaces. Knowing the delay between the emission and the reception of the ultrasonic waves and the velocity of the wave through the medium under consideration, it is possible to determine the thickness of the layer.

However, for a deposit growing on a membrane, the velocity of the ultrasonic wave is not known. Thus, the thickness of the deposited layer has to be calculated by comparing, at a given time, the flight time of the echo created at the fouling layer surface (flight time between the transducer and the fouling layer) with the initial flight time of the echo formed on the clean membrane (flight time between the transducer and the clean membrane). More details are given elsewhere [5]. A transducer with a frequency of 20 MHz was used. The thickness of the fouling was determined with an uncertainty of 10%.

3. Results

3.1. Thickness of the calibrated test piece

Measurements of the difference of thickness between notches 1 and 3 were made using the two methods. The results obtained with each method are shown in Table 1. A comparison is provided with values given by a sensor gauge.

Considering the measurement precision, these results show that the thicknesses obtained with the LSGI and UTDR methods were comparable to those measured using a sensor gauge. The low precision obtained for the laser triangulometry was due to the use of a lens with a lower magnification than the one used during the filtration test (12 X against 24 X). This choice was justified by the necessity to visualize the whole piece on a single image.

From to these results, it can be concluded that these methods are relevant for measuring the thickness of a rigid, continuous medium with a well defined interface.

3.2. Filtration experiments

3.2.1. Flux decline

The feed suspension of spherical melamine particles was filtered on two different membranes at a transmembrane pressure of 1 bar. Each measurement was performed several times. Typical variations of flux versus deposited mass of particles during filtration are presented, for both membranes, on Fig. 2.

When the suspension was filtered on the 100 kDa membrane, the flux declined from its initial value of 360 l/h.m² to 230 l/h.m² for a deposited mass of 145 g/m². This corresponded to a total flux loss of about 50% during the filtration run. Note that the sudden flux variations observed at the beginning of the experiment (for deposited masses around 15 and 60 g/m²) were due to small transmembrane pressure variations (less than 0.02 bar) during the filtration run. During suspension

Table 1
Comparison of difference of thickness of notches 1 and 3 determined by LSGI and UTDR method with value measured from the sensor gauge

Method	Sensor gauge	LSGI	UTDR
Δe (μm)	513 ± 8	493 ± 75	502 ± 8

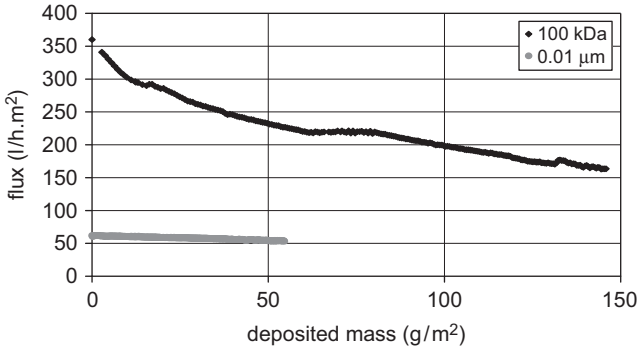

Fig. 2. Flux variation during filtration (TMP = 1 bar) of melamine suspension (C = 0.15 g/l) against mass deposited on the membrane area for 100 kDa membrane (LP0 = 360 l/h.m².bar) and membrane with a pore size of 0.01 µm (LP0 = 62 l/h.m².bar).

filtration on the 0.01 µm membrane, the flux declined linearly from an initial value of 62 l/h.m² to 54 l/h.m² for a final deposited mass of 55 g/m². This variation corresponded to a total flux loss of 9%. Thus, the flux decline was more pronounced for the 100 kDa MWCO membrane than for the 0.01 µm one.

3.2.2. Fouling layer thicknesses

During a filtration run, fouling layer thicknesses were measured simultaneously by UTDR and LSGI at the same location. The ultrasonic transducer was placed at less than two centimeters from the surface characterized by the LSGI method. The thicknesses obtained by both methods during filtration on the two different membranes are shown on Fig. 3.

From Fig. 3 (a), it can be seen that, during filtration on the 100 kDa membrane, the fouling layer grew continuously with particle deposition. At the end of the experiment, for a deposited mass of 145 g/m² the thickness of the cake layer was about 65 µm. It is also clear that LSGI and UTDR give the same results. Thus, the interface between the bulk suspension and the fouling layer determined by both methods is located at the same position.

In Fig. 3 (b), the thicknesses of the fouling layer formed on membrane with a pore size of 0.01 µm differ. For a deposited mass of melamine of 50 g/m², LGSI indicates a thickness of 89 µm, while it is only 63 µm for UTDR. Thus, the optical method gives a thickness 1.4 times that given by the acoustic one. However, the variation of thickness with time determined by both methods exhibits the same trend on both curves.

The fouling layer growth kinetics can also be studied. Fig. 4 represents the fouling layer relative thickness (defined as the ratio of its thickness at a given time to its final thickness) versus the amount of particles deposited for filtration on a membrane with a pore size of 0.01 µm.

The growth kinetics are not constant in time. After a rapid growth of the fouling layer (50% of the total thickness is reached for a deposited mass of around 20 g/m²), the increase becomes linear and the other 50% of the cake layer height is built up by the deposit of a further 30 g/m² on the membrane surface. However, although the growth kinetics are not constant in time, LSGI and UTDR indicate the same kinetic growth.

Thus, it can be seen from these results that, in the case of 100 kDa membrane with high permeability (360 l/h.m².bar), the thicknesses given by both methods are the same. However, for a less permeable membrane (62 l/h.m².bar) the thicknesses given by UTDR and LSGI differ. Nevertheless, the growth kinetics values calculated from the two methods are the same.

As the measurements were performed using waves (optical electromagnetic waves and ultrasonic mechanical waves) the results are directly related to the behavior

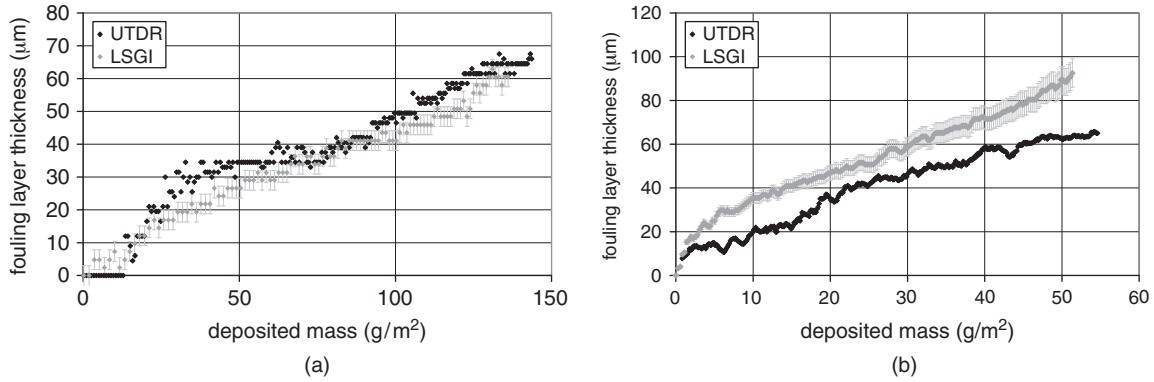

Fig. 3. Fouling layer growth during filtration (TMP = 1 bar) of melamine suspension (C = 0.15 g/l) on (a) 100 kDa membrane (LP0 = 360 l/h.m².bar) and (b) membrane with a pore size of 0.01 µm (LP0 = 62 l/h.m².bar).

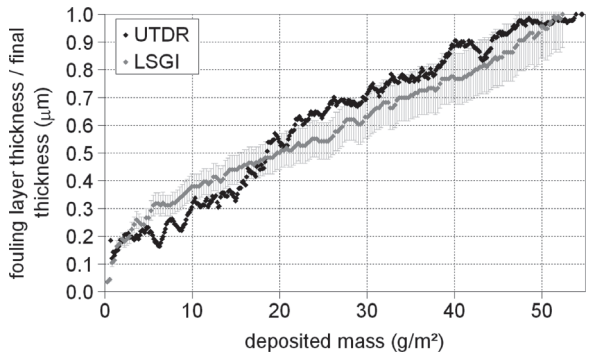

Fig. 4. Fouling layer relative thickness against mass deposited on membrane area during filtration of melamine suspension on 0.01-μm –pore-size membrane (C = 0.15 g/l, LP0 = 62 l/h.m².bar, TMP = 1 bar).

of the waves at the interface between the feed suspension and the fouling layer. Thus, the physical properties (density, porosity, etc.) of the fouling layer have a direct impact on the measurement. Consequently, to understand the differences in results found using LSGI and UTDR under different hydrodynamic conditions, it is necessary to examine the properties of the fouling layers.

3.2.3. Structural properties

For a given fouling layer thickness of melamine particles, the fouling layer resistance is dependent on its structural properties. The denser the fouling layer is, the more resistance it opposes to the mass transfer of fluid through it.

In order to compare structural properties of the two fouling layers formed on 100 kDa and 0.01 μm membranes, the fouling layer resistances were plotted versus the thicknesses measured by the two methods (Fig. 5). The fouling layer resistances, calculated using Darcy's relation, are a global parameter related to fouling layer properties.

Whatever the method used to measure the fouling thickness, for a given thickness, fouling layers formed on the two membranes showed different resistances. For a layer measured as 50 μm by the optical method, the fouling layer formed on the more permeable membrane had a resistance of around 11 x 10^{11} m^{-1} as against 2.7 x 10^{11} m^{-1} for filtration performed on the less permeable membrane. In the case of the 100 kDa membrane, the 50 μm fouling layer was thus four times as resistant as the one formed on the 0.01 μm membrane. Looking at values determined by UTDR, the resistance difference is smaller. Thus, for a 50 μm thickness, the fouling layer formed on the 100 kDa membrane had a resistance of 10 x 10^{11} m^{-1}, as compared to 4 x 10^{11} m^{-1} when the membrane with 0.01 μm pore size was used.

Thus, for a given thickness, the fouling layer formed on the 100 kDa membrane was more resistant than the one formed on the second membrane. These results indicate that the two layers did not have the same structure and that the fouling layer formed on the 100 kDa membrane was more compact than the one formed on membrane with a pore size of 0.01 μm.

Cleaning efficiency of the fouled membrane is directly linked to fouling layer properties. So, this parameter was also studied. After a relaxation phase, a flush was performed to remove dispersed particles. After this step, if the initial membrane permeability was not recovered, a backwash was performed. The results obtained in terms of permeability recovery are summarized below (Table 2).

From these results, one can see that, in the case of 0.01 μm membrane, the relaxation period followed by a flush was sufficient to recover the initial membrane permeability. Particles were loosely linked to the

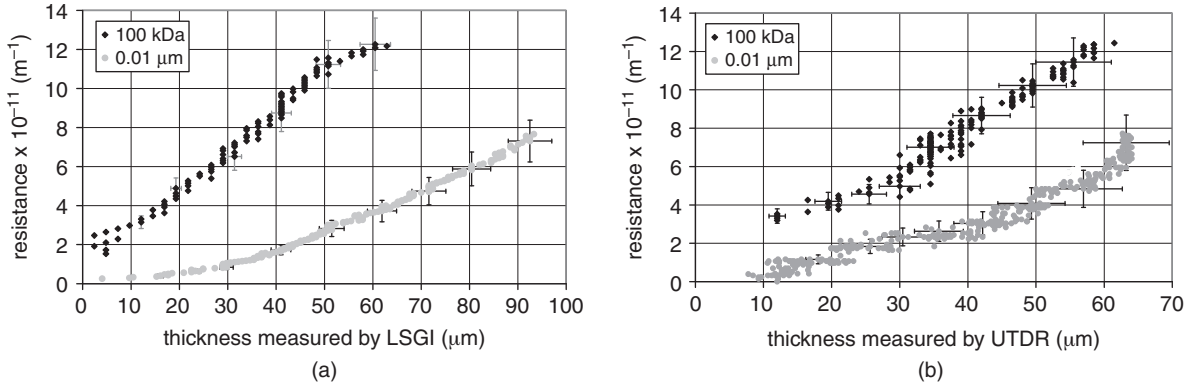

Fig. 5. Fouling layer resistance variation against layer thickness determined during filtration on 100 kDa membrane (LP0 = 360 l/h.m².bar) and 0.01μm pore size membrane (LP0 = 62 l/h.m².bar) (C = 0.15 g/l, PTM = 1 bar) by (a) LSGI (b) UTDR.

Table 2
Cleaning protocol and efficiency in terms of permeability recovery

Membrane type	Final deposited mass (g/m²)	Cleaning protocol	Initial permeability (l/h.m².bar)	Permeability after cleaning (l/h.m².bar)	Lpf/Lp_0 (%)
0.01 µm	55	Relaxation + flush	62	62	100
100 kDa	145	Relaxation + flush + backwash	360	262	73

membrane since no backwashing was needed. For the 100 kDa membrane, these two steps were not sufficient to recover the membrane initial permeability and a third step of backwashing was performed. The fouling layer was thus more strongly linked to the membrane as a backwash was needed.

The necessity of using two different cleaning protocols, and although the masses deposited on the two membranes were not the same, clearly indicates that the two layers have different structures. These data are consistent with the fact that the fouling layer formed on the 100 kDa membrane was more compact than the one formed on the less permeable membrane.

4. Discussion

Cleaning efficiency results together with fouling layer resistance at a given thickness showed that two layers of different natures were formed. In the case of the 100 kDa membrane (LP_0 = 360 l/h.m².bar) the layer was compact and interacted strongly with the membrane. The fouling layer could be considered as a cake layer with a well defined interface. However, in the case of the membrane with pore size of 0.01 µm (LP_0 = 62 l/h.m².bar), the layer was more porous, and easily removable. This tends to indicate that this fouling layer was due to polarization concentration rather than being a deposit layer.

Furthermore, comparing the two filtration runs, a ratio of about 6 was found between the initial permeabilities of the two membranes (360 l/h.m².bar against 62 l/h.m².bar). Thus, in the case of the 100 kDa membrane, the convective force was about six times as large as for the less permeable membrane. Consequently, if a mass balance is applied on a particle, particle-particle repulsions are likely to have greater importance for keeping the particle in suspension. This is consistent with observations and could explain the differences in fouling layer properties.

As the nature of the interaction between particles and waves really depend on the particulate layer structure, the different results obtained when measuring the fouling layer thickness can be explained by the different natures of the fouling layers. Thus, the position of the interface where the waves (acoustic or optical ones) interact with the fouling layer depends not only on the particle shape, size and roughness but also on its volumetric concentration. In case of interaction of waves with a layer containing a concentration gradient, the position of the interface between the bulk suspension and the layer will also be very dependent on the wavelength. Consequently, in the case of a porous layer with a large concentration gradient, such as a concentration polarization layer, optical and acoustic layers are likely not to interact at the same depth of the fouling layer, thus leading to the formation of two different interfaces. This explains the difference of thickness observed in the case of melamine filtration on the membrane with the pore size of 0.01 µm.

5. Conclusion

This study has demonstrated that the LSGI and UTDR methods are validate for measuring the thickness of a rigid, continuous medium with a well defined interface. Additionally, for a compact porous layer with a clear interface, both methods give the same thickness. However, for a layer with high porosity and a concentration gradient, such as a polarized layer, the interface between the feed suspension and the fouling layer is not the same for both methods. Nevertheless, both methods give the same growth kinetics.

Thus, LSGI and UTDR are two complementary methods which, depending on the operating conditions, determine fouling layer thickness and/or its growth kinetics.

Acknowledgement

This study was supported by the French National Agency for research (ANR) (FiltraCOPPE project).

References

[1] A.P. Mairal, A.R. Greenberg, W.B. Krantz and L.J. Bond, Real-time measurement of inorganic fouling of RO desalination membranes using ultrasonic time-domain reflectometry, J. Membr. Sci., 159(1–2) (1999) 185–196.

[2] V. Chen, H. Li and A.G. Fane, Non-invasive observation of synthetic membrane processes – a review of methods, J. Membr. Sci., 241(1) (2004) 23–44.

[3] P. Le-Clech, Y. Marselina, Y. Ye, R.M. Stuetz and V. Chen, Visualisation of polysaccharide fouling on microporous membrane using different characterisation techniques, J. Membr. Sci., 290(1–2) (2007) 36–45.

[4] J. Mendret, C. Guigui, P. Schmitz, C. Cabassud and P. Duru, An optical method for in situ characterization of fouling during filtration, AIChE, 53(9) (2007) 2265–2274.

[5] X. Xu, J. Li, H. Li, Y. Cai, Y. Cao, B. He and Y. Zhang, Non-invasive monitoring of fouling in hollow fiber membrane via UTDR, J. Membr. Sci., 326(1) (2009) 103–110.

[6] J. Mendret, C. Guigui, C. Cabassud, N. Doubrovine, P. Schmitz, P. Duru, J.-Y. Ferrandis and D. Laux, Development and comparison of optical and acoustic methods for in situ characterisation of particle fouling, Desalination, Volume 199, Issues 1–3, Euromembrane 2006, (2006), 373–375.

[7] I.S. Ngene, R.G.H. Lammertink, M. Wessling and W. van der Meer, A microfluidic membrane chip for in situ fouling characterization, J. Membr. Sci., 346(1) (2010) 202–207.

[8] J. Mendret, C. Guigui, C. Cabassud, P. Schmitz, Numerical investigations of the effect of non-uniform membrane permeability on deposit formation and filtration process, Desalination, 263(1–3), (2010), 122–132

[9] Y. Bessiere, N. Abidine and P. Bacchin, Low fouling conditions in dead-end filtration: Evidence for a critical filtered volume and interpretation using critical osmotic pressure, J. Membr. Sci., 264(1) (2005) 37–47.